ELSEVIER

Ultrasound in Med. & Biol., Vol. 24, No. 4, pp. 503–511, 1998

0301-5629/98 $19.00 + .00

PII S0301-5629(98)00019-2

● *Original Contribution*

EFFECTS OF A SUDDEN FLOW REDUCTION ON RED BLOOD CELL ROULEAU FORMATION AND ORIENTATION USING RF BACKSCATTERED POWER

ZHAO QIN,[†‡] LOUIS-GILLES DURAND,[†‡] LOUIS ALLARD,[†] GUY CLOUTIER[†‡]

[†]Laboratory of Biomedical Engineering, Institut de recherches cliniques de Montréal, Montréal, Canada; and
[‡]Department of Medicine, University of Montréal, Montréal, Canada

(*Received* 9 *September* 1997; *in final form* 29 *January* 1998)

Abstract—In most studies that were aimed at evaluating the kinetics of red blood cell (RBC) aggregation, human blood was initially circulated at a high shear rate to disrupt the aggregates, and measurements were performed following a complete flow stoppage, during the process of rouleau formation. However, it is known that a very low shear rate can enhance the formation of aggregates, as demonstrated by the modal relationship of the shear-rate dependence of RBC aggregation. The objective of the present study was, thus, to evaluate the influence of sudden flow reductions compared to a complete flow stoppage on the kinetics of rouleau formation, using ultrasound backscattering. Horse blood models, characterized by different aggregation levels, were obtained by diluting the plasma with a saline solution in different proportions. Blood was circulated in a 12.7-mm vertical tube at a flow rate of 1250 mL min^{-1} (prereduction flow rate) to disrupt the aggregates. The ultrasound radiofrequency (RF) signal was recorded from the center of the tube following different levels of sudden flow reduction or complete stoppage (postreduction flow rate). All measurements were performed over 2 min, using a 10-MHz transducer. No power increase was observed after complete flow stoppage. For postreduction flow rates varying between 20 and 160 mL min^{-1}, the backscattered power increased proportionally with the kinetics of RBC aggregation. The echo buildup was also faster and stronger when the postreduction flow rate was increased. An unexpected pattern of variation of the backscattered power was found for horse RBCs characterized by high kinetics of rouleau formation. The power increased rapidly to a plateau, followed by another rapid increase and another plateau. Rouleau formation, random disorientation and reorientation were postulated to explain the phasic power increases observed. © 1998 World Federation for Ultrasound in Medicine & Biology.

Key Words: **Acoustic backscattering, Red blood cell aggregation, Biorheology, Ultrasound radiofrequency backscattered power, Pulse-echo, A-mode, Kinetics of rouleau formation.**

INTRODUCTION

Red blood cell (RBC) aggregation is a normal reversible physiological process occurring in flowing blood. As shown by Chien (1976) and Copley et al. (1976), the shear rate dependence of RBC aggregation is described by a modal function (a function with a single maximum). Under static conditions, RBC aggregates exist, but a slight increase of the shear rate enhances the interactions between RBCs and, consequently, the level of aggregation. For a given blood sample, the shear rate at which the aggregation is maximum (the maximum of the modal function) varies as a function of the kinetics of rouleau formation, which depends on the hematocrit, the temperature, the concentration and affinity of plasma adhesion macromolecules, and the characteristics of the RBC membrane. The dispersion of the aggregates occurs under high shear rate conditions. Because RBC aggregation is a reversible process, rouleaux are formed again if the shear rate is reduced.

Because of its sensitivity to the presence of RBC aggregates, ultrasound backscattering was used to characterize the kinetics of RBC rouleau formation. The kinetics of rouleau formation refers here and hereafter to the increase in rouleau size per unit of time. Shung and Reid (1979) used a 7.5-MHz ultrasound transducer to record the time variation of the backscattering amplitude from human blood samples at a low hematocrit (8.2%), after flow stoppage. They showed that the backscattering amplitude increased initially after stoppage and reached a plateau in

Address correspondence to: Dr. Guy Cloutier, Laboratory of Biomedical Engineering, Institut de recherches cliniques de Montréal, 110 avenue des Pins Ouest, Montréal, Québec H2W 1R7 Canada. E-mail: cloutig@ircm.umontreal.ca

about 2–4 min. At high plasma fibrinogen concentrations, the backscattering amplitude increased more rapidly and the final value was higher than that found at lower concentrations. Boynard et al. (1987) also showed that the ultrasound backscattering coefficient at 6 MHz increased with time after stopping the stirring of human blood. By measuring changes in the backscattered power during 20 min after flow stoppage, their study also included the phase of sedimentation of RBC aggregates.

Using a 10-MHz B-mode ultrasound scanner, Kim et al. (1989) observed that the increase in echogenicity of human blood occurs mainly within the first 140 s after flow stoppage. Following that period, the power continued to increase slowly for up to 4 min. The increase in echogenicity per unit of time was inversely proportional to the hematocrit for hematocrits between 15% and 60%. They concluded, from their study, that ultrasound echogenicity is a measure of the degree of aggregation for a given hematocrit. Based on the spectral analysis of the RF ultrasound signal, Kitamura et al. (1995) studied human RBC aggregate formation as a function of time following flow stoppage for different fibrinogen concentrations and hematocrits. At a constant hematocrit of 40%, rouleau buildup was proportional to the fibrinogen concentration. At a constant fibrinogen concentration, the aggregate size reached similar levels by varying the hematocrit, but the rates of increase were inversely proportional to the hematocrit. From these observations, they suggested that the hematocrit may determine the rate of aggregate formation and the fibrinogen concentration, the size of aggregates. In a recent study (Weng et al. 1997), it was shown that fibrinogen affects, not only the size, but also the adhesive forces between RBCs and the rate of rouleau formation.

In previous studies, blood flow was always stopped after dispersing RBC aggregates at a high flow rate for several min. However, as previously mentioned, a very low shear rate can promote the enhancement of RBC aggregation. Therefore, a sudden reduction of the flow, instead of a complete stoppage, may better enhance RBC aggregation. The objective of the present study was to evaluate the influence of the postreduction flow rate on the kinetics of rouleau formation using ultrasound backscattering. Horse blood models characterized by different levels of RBC aggregation kinetics were used. Carbon fibers were also circulated in the flow model to study the influence of different levels of flow reduction and complete stoppage on the orientation of the particles.

MATERIALS AND METHODS

Kinetics of RBC rouleau formation

All measurements were performed within 48 h after EDTA anticoagulated horse blood collection. Before each experiment, the plasma was separated from the red and white cells by sedimentation. Several blood samples of 1.5 mL were prepared by replacing a part (between 0 and 75%) of the total volume of plasma with an isotonic NaCl solution. Using diluted plasma, different RBC aggregation kinetics were obtained because of the reduction of the concentration of plasma proteins responsible for the aggregation (Weng et al. 1996). The kinetics of rouleau formation was measured from these samples at room temperature and 40% hematocrit using an erythroaggregameter based on a Couette flow system (Regulest, Florange, France). A laser diode (Hitachi, HL7801G) providing a radiation at 780 nm was used as the light source. An index S_{10} reflecting the kinetics of rouleau formation was derived from the analysis of the variations in light intensity of the signal reflected by blood (Donner et al. 1988). S_{10} has a direct relationship with the kinetics of aggregation and was computed as the ratio of the area above the light intensity curve during the first 10 s after stoppage of the rotation of the cylinder to the total area within the same period of time. A shear rate of 550 s^{-1} was used before flow stoppage to disrupt rouleaux of RBCs.

Five horse blood models from different animals were prepared by selecting the appropriate plasma dilution level. Samples with values of S_{10} of 11.2, 14.8, 18.9, 25.6 and 32.3 were used. For each experiment, 1.5 L of blood was reconstituted, using each dilution level selected, and circulated into the flow model for at least 0.5 h before beginning the experiment. This procedure eliminated air bubbles and allowed the temperature of blood to reach that of the ambient air. The aggregation indices were measured again during the experiment from a sample of 1.5 mL taken from the flow model. Mean values are reported in this manuscript.

Measurements with a suspension of carbon fibers

Carbon fibers were circulated in the flow model to study the influence of the fiber orientation on the ultrasound backscattered power following flow reductions. Cylindrical carbon fibers (Goodfellow, Berwyn, PA) with a mean radius of 7 μm and a mean length of 250 μm were suspended in a test fluid made of a volume of 40% glycerol and 60% saline at a concentration of 0.5 g L^{-1}. Carbon fibers were previously used as scatterers in a flow loop model (Allard et al. 1996) and in a tissue-mimicking phantom (Mottley and Miller 1988). The results of the experiments with carbon fibers were compared to those obtained with horse blood. Because the size (radius and length) of the fibers is independent of the flow conditions, the results obtained with carbon fibers should distinguish between the influence of the particle orientation on the

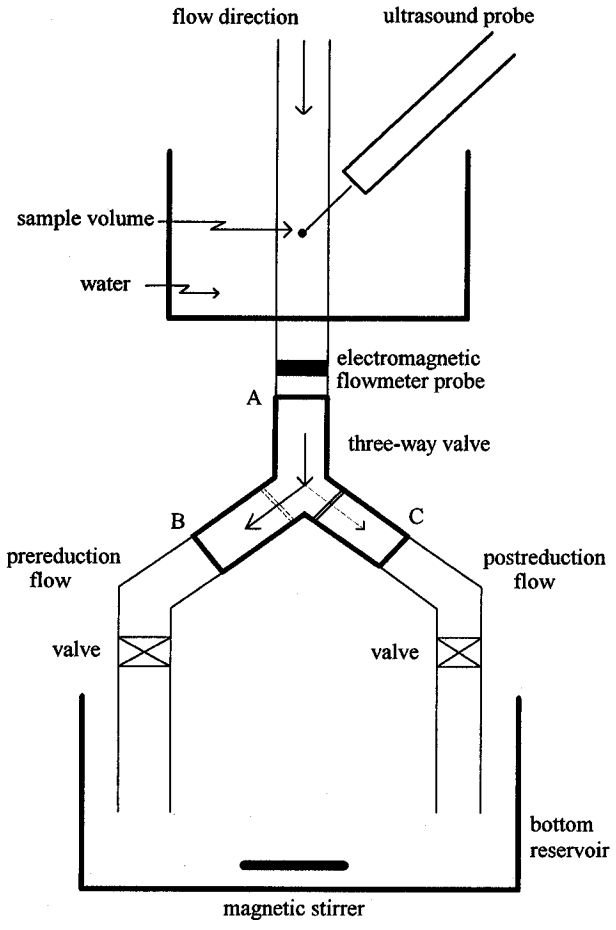

Fig. 1. Schematic representation of the flow loop model used to change the flow rate from the prereduction to the postreduction levels.

backscattered power and that associated with the binding of rouleaux and dynamic rouleau buildup.

Flow loop model

The steady-flow loop model described in detail by Cloutier et al. (1996) was modified according to Fig. 1. To change the flow rate rapidly from the prereduction state to the postreduction rate, a 3-way valve was used. In valve position A–B, blood flow circulated in the left branch at a prereduction flow rate of 1250 mL min^{-1} (maximum centerline velocity $\approx$ 26 cm/s). In position A–C, blood was circulated in the right branch at postreduction flow rates varying between 20 and 160 mL min^{-1}. Two other valves were used in the model to adjust the prereduction and postreduction flow rates. In position B–C, the flow was immediately stopped, resulting in a postreduction flow rate of zero. The carbon fiber suspension was circulated at 1000 mL min^{-1} before reducing the flow to values varying between 0 and 250 mL min^{-1}.

The flow model was composed of a peristaltic pump, a vertical Kynar tube with an inside diameter of 12.7 mm, a bottom reservoir of 2 L and a top reservoir used to minimize the oscillations produced by the pump. A cannulating type flow probe was inserted into the flow tubing to measure the flow rate with an electromagnetic blood flowmeter (Carolina Medical Electronics, Cliniflow II, model FM701D, King, NC). A magnetic stirrer was used to continuously mix blood or the suspension of carbon fibers in the bottom reservoir. The peristaltic pump circulated the fluid from the bottom to the top reservoir. To allow acoustic coupling, the ultrasound transducer was immersed in a small tank filled with distilled water. The transducer was held at an angle of 45° to the flow direction. RF ultrasound measurements were performed at the center of the tube. The Doppler frequency shift was used to position the sample volume at the center of the tube before reducing the flow.

Narrow-band RF signal acquisition and processing

The RF backscattered ultrasound signal was obtained by using a 3 mm × 3 mm transducer connected to a 10-MHz pulse-wave Doppler system developed at the Baylor College of Medicine. An electronic driver circuit was built in the system to allow the acquisition of the RF signal before quadrature demodulation. The duration of the transmitted ultrasonic bursts was 0.8 μs (8 cycles). To reduce the bandwidth and increase the signal-to-noise ratio, an elliptic band-pass filter centered around 10 MHz (BP-10.7, Mini-Circuits, Brooklyn, NY) was inserted between the ultrasound system and the input of the data-acquisition board. The insertion loss of this filter was 0.86 dB at 10.7 MHz, its pass-band was from 8.5 to 12.7 MHz at −3 dB, and from 7.6 to 14.4 MHz at −20 dB. As reported in the Appendix, the electronic circuits had a linear response over the whole range of backscattered power measured with the different blood models and carbon fiber solutions.

To allow successive recordings of the pulse-wave signal during a period of 2 to 4 min following flow reductions, a time gating circuit was designed to reduce the pulse-repetition frequency (*PRF*) of the instrument and control the gate duration from which the backscattered echoes were detected. The RF signal was digitized at a sampling frequency (F_s) of 100 MHz with 8-bit resolution by a Gagescope acquisition board (model 250-4 MB, Montreal, Quebec, Canada). The gated data acquisition mode was used with the Gagescope board to digitize signals only when the gate corresponding to the position of the sample volume was on. The RF signals were sampled using a *PRF* of 250 Hz and a gate duration (t_g) of 0.5 μs. After data acquisition, the backscattered RF signal of each experiment was separated in measure-

ment intervals (M) from which the mean power (P), expressed in dB, was calculated by:

$$P = 10 \times \log\left(\frac{1}{N}\sum_{k=1}^{N} V_k^2(t)\right), \quad (1)$$

where N corresponds to $M \times F_s \times t_g \times PRF$, and $V_k(t)$ is the ultrasound RF signal. The measurement interval M was set at 1 s for horse blood and 10 s for carbon fibers. For measurements with horse blood, P values were calculated over 120 nonoverlapping windows (sampling duration of 2 min), whereas 24 nonoverlapping windows (sampling duration of 4 min) were used for carbon fibers. To reduce fluctuations in the mean ultrasound backscattered power curves, a 5-point smoothing filter was used. For each experiment, measurements were repeated 5 times for statistical averaging.

Statistical analyses

Two-way analyses of variance (SigmaStat, version 1.0, Jandel Scientific, San Rafael, CA) were used to confirm the influence of time and aggregation kinetic index S_{10} on the backscattered power. For experiments performed on the same blood sample using different postreduction flow rates, 2-way repeated-measures analyses of variance were used to assess the effect of time and flow rate on the backscattered power. A significance level of 5% was used in all analyses.

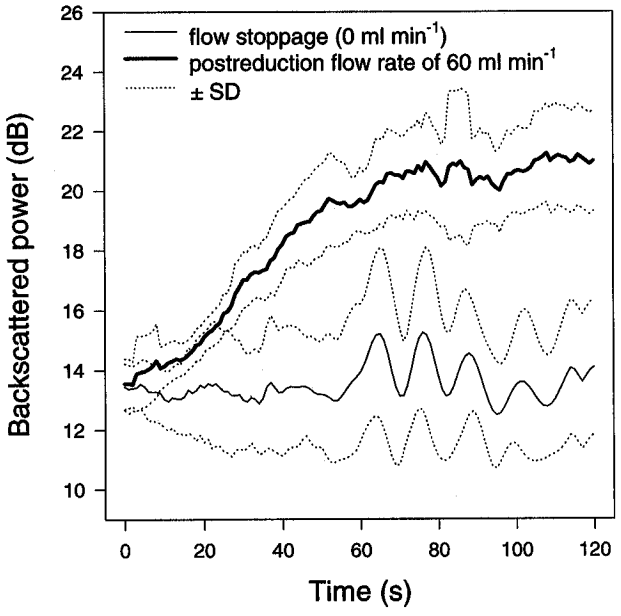

Fig. 2. Mean ± standard deviation (SD) of the ultrasonic backscattered RF power increase following a sudden flow stoppage and a flow rate reduction to 60 mL min^{-1} for a horse blood model characterized by S_{10} of 14.8. The prereduction flow rate was 1250 mL min^{-1} for both measurements. For each curve, averaging was performed over 5 measurements.

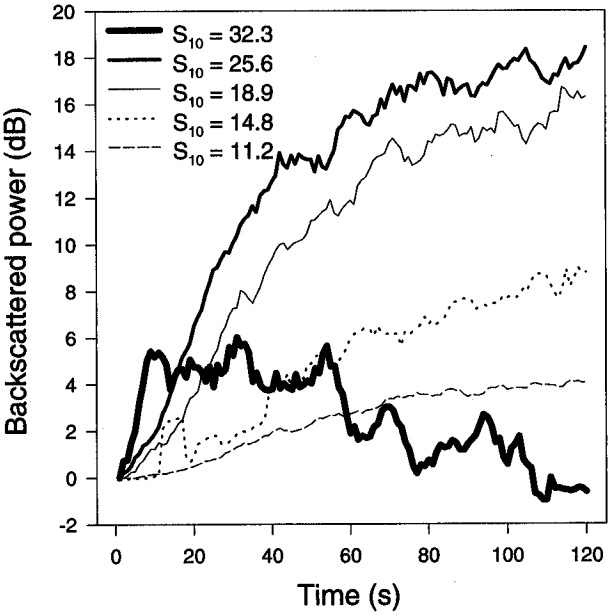

Fig. 3. Ultrasonic backscattered RF power increase following a sudden flow rate reduction from 1250 to 40 mL min^{-1} for horse blood models characterized by five levels of RBC aggregation kinetic indices S_{10}. For each curve, averaging was performed over 5 measurements.

RESULTS

Figure 2 shows the mean ± one standard deviation (SD, $n = 5$) values of the backscattered power[1] for measurements characterized by postreduction flow rates of 0 and 60 mL min^{-1} and an aggregation kinetic index S_{10} of 14.8. No significant increase ($p > 0.05$) in power was observed as a function of time following complete flow stoppage. For a postreduction flow rate of 60 mL min^{-1}, the power increased progressively from 13.6 to 21.2 dB ($p < 0.0001$). The postreduction flow rate had a significant effect ($p = 0.0002$) on the backscattered power. Figure 3 shows the variation of the backscattered power following a sudden flow reduction to 40 mL min^{-1} for horse blood, with five different aggregation kinetic indices. The power values measured immediately after flow reduction were normalized to 0 dB to allow relative comparisons. As seen in this Fig., the range of variations of the backscattered power increased progressively with time for S_{10} varying between 11.2 and 25.6

[1] The standard deviations shown in Fig. 2 were similar for all other experiments performed and only mean values are presented in other figures.

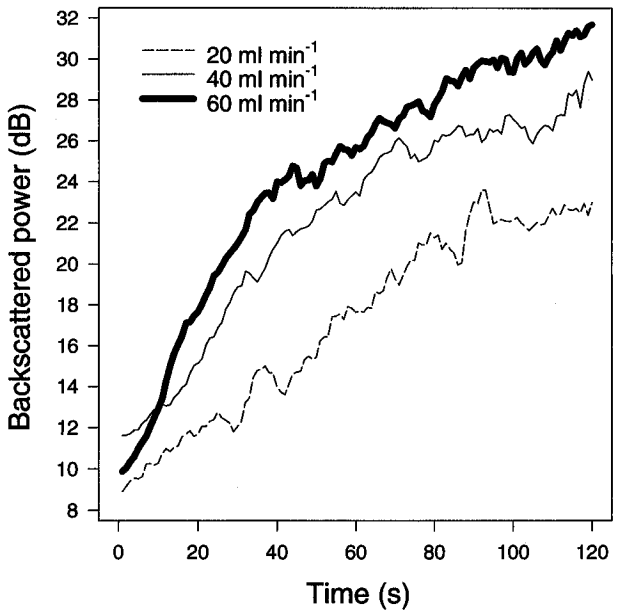

Fig. 4. Ultrasonic backscattered RF power increase following a sudden flow rate reduction from 1250 mL min^{-1} to postreduction flow rates of 20, 40 and 60 mL min^{-1}. The RBC aggregation kinetic index S_{10} for those measurements was 25.6. For each curve, averaging was performed over 5 measurements.

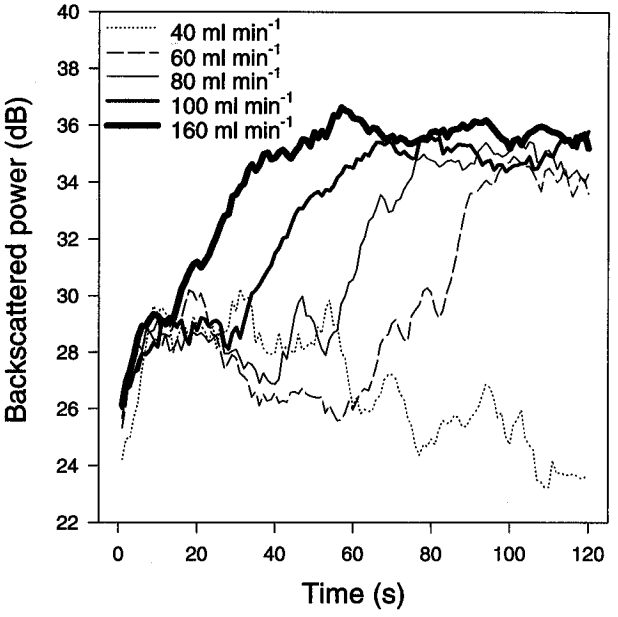

Fig. 5. Ultrasonic backscattered RF power increase following a sudden flow rate reduction from 1250 mL min^{-1} to postreduction flow rates of 40, 60, 80, 100 and 160 mL min^{-1}. The RBC aggregation kinetic index S_{10} for those measurements was 32.3. For each curve, averaging was performed over 5 measurements.

($p < 0.0001$). Following 2 min of flow reduction, a 3.7 dB power increase was observed for $S_{10} = 11.2$, whereas the power increase reached 18 dB for $S_{10} = 25.6$. For $S_{10} = 32.3$ (the highest RBC aggregation kinetics tested), the power variation as a function of time was statistically significant, but did not follow the general tendency observed for lower aggregation indices. All pairwise comparisons of the backscattered power curves for the aggregation kinetics tested were statistically significant ($p < 0.0001$).

It was observed that the postreduction flow rate had an effect on the power variation. As seen in Fig. 4 for $S_{10} = 25.6$, increasing the postreduction flow rate from 20 to 60 mL min^{-1} resulted in larger power increases at 2 min and steeper slopes within the first 20 to 40 s. Each backscattered power curve presented statistically significant variations as a function of time ($p < 0.0001$). Except for the comparison between postreduction flow rates of 40 and 60 mL min^{-1}, all other pairwise comparisons of the backscattered power curves were statistically significant ($p < 0.01$). For $S_{10} = 32.3$ (Fig. 5), a different behavior was found. For the postreduction flow rate of 40 mL min^{-1}, the power increased rapidly by 5.4 dB within the first 10 s, reached a plateau, and dropped between 55 and 120 s, approximately. For all other postreduction flow rates, the power increased rapidly, dropped slowly before reaching a plateau, and then increased again before reaching another plateau. The duration between the two phases of rapid power increase seemed to be inversely related to the postreduction flow rate. The same level of power was attained in the second plateau for postreduction flow rates varying between 60 and 160 mL min^{-1}. Because the interval between the two phases of power increase is enlarged when the flow rate is reduced, it is expected that a similar behavior might occur beyond 2 min for the postreduction flow rate of 40 mL min^{-1}. In Fig. 5, both time ($p < 0.0001$) and postreduction flow rate ($p < 0.05$) had a significant effect on the backscattered power. Figure 6 shows the variation of the backscattered power using carbon fibers. For all postreduction flow rates tested, a fast power decrease was observed within the first seconds, followed by a tendency toward a power increase. The time interval corresponding to the fast decrease in power and the maximum power reduction was inversely proportional to the postreduction flow rate. All three power curves presented statistically significant variations as a function of time ($p < 0.0001$). Except for the comparison between postreduction flow rates of 150 and 250 mL min^{-1}, all other pairwise comparisons of the backscattered power curves were statistically significant ($p < 0.05$).

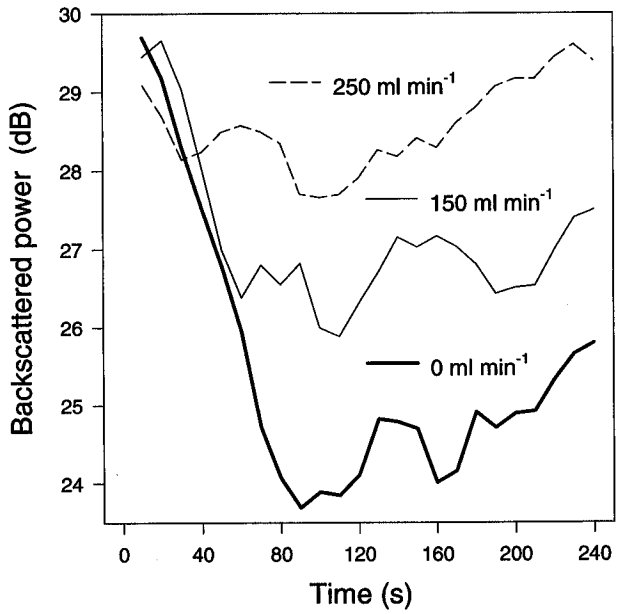

Fig. 6. Ultrasonic backscattered RF power variation following a sudden flow stoppage and reduction from 1000 mL min^{-1} to postreduction flow rates of 0, 150 and 250 mL min^{-1} using a suspension of carbon fibers. For each curve, averaging was performed over 5 measurements.

DISCUSSION

Plasma-diluted horse blood was used to stimulate the kinetics of normal, hypo-, and hyperaggregating RBCs. At 37°C, the mean value of S_{10} for normal human blood is 23 ± 3 (n = 19) (Weng et al. 1996). In the present study, S_{10} ranged between 11.2 (hypoaggregation kinetics) and 32.3 (hyperaggregation kinetics). Interesting behaviors not reported in previous studies by using normal human RBCs were observed.

The influence of the level of RBC aggregation kinetics

With the exception of S_{10} = 32.3, both the rate of increase of the backscattered power and the power variation within 2 min of flow reduction were proportional to the RBC aggregability (see Fig. 3). Both parameters can, thus, predict the kinetics of RBC aggregation. However, because the prereduction flow rate can affect the backscattered power at t = 0 (Cloutier et al. 1996), the range of power increase may vary if insufficient shearing is used to disrupt rouleaux. For this reason, the rate of increase of the power may be a better index to assess the kinetics of rouleau formation. The specific pattern of variation of the backscattered power for hyperaggregating RBCs (S_{10} = 32.3) is discussed later.

The influence of the postreduction flow rate

In previous studies evaluating the kinetics of RBC aggregation with ultrasound (Shung and Reid 1979; Boynard et al. 1987; Kim et al. 1989; Kitamura et al. 1995), human blood was initially sheared to disperse the aggregates, the flow was then completely stopped, and the echogenicity or RF backscattered power measured during several min. As shown in these studies, the backscattered power increased as a function of time and the range of variation had an inverse relationship with the hematocrit for hematocrits lower than 43%. At a high hematocrit of 60%, no power increase was observed as a function of time (Kim et al. 1989; Kitamura et al. 1995).

In the present study, with horse blood at 40% hematocrit, stopping the flow did not produce significant power increases over 2 min. The difference in the kinetics of rouleau formation between normal human and horse RBCs at 40% hematocrit can be explained by the modal shear-rate dependence of RBC aggregation. As summarized in the Introduction, this modal function suggests that increasing the shear rate from zero up to a given value promotes rouleau formation. The shear rate that produces the maximum aggregation differs between species and blood samples. By increasing the shear rate beyond that producing the maximum aggregation, rouleaux are disrupted. According to a recent study by our group (Qin et al. 1998), shearing between 1 and 25 s^{-1} is necessary to enhance rouleau formation with horse blood. For normal human blood, shearing between 0.5 and 1 s^{-1} is sufficient to promote rouleau buildup (Chien 1976). These differences in the maximum shear rate promoting rouleau formation explain the differences observed between our results and results reported in the literature at 40% hematocrit following complete flow stoppage (Shung and Reid 1979; Boynard et al. 1987; Kim et al. 1989; Kitamura et al. 1995).

In the present study, stopping the flow did not provide the shearing necessary to promote rouleau buildup with horse blood. However, increasing the postreduction flow rate significantly increased the degree of shearing and, consequently, the backscattered power. With normal human blood (Shung and Reid 1979; Boynard et al. 1987; Kim et al. 1989; Kitamura et al. 1995), it is possible that the residual kinetic energy of the flow after stoppage, vibration of the flow model and Brownian motion provided enough shearing to promote an increase in the ultrasound backscattered power. The absence of power increase at 60% hematocrit found by Kim et al. (1989) and Kitamura et al. (1995), may be explained by a shift to a higher value of the maximum of the modal shear rate function.

In the present study, a postreduction flow rate was always necessary to observe backscattered power increases. As seen in Fig. 4, few differences in the backscattered power were observed at the beginning of the postreduction phase. However, the echo buildup was faster and the power at 2 min was stronger when the

postreduction flow rate was increased from 20 to 60 mL min^{-1}, indicating a higher kinetics of aggregation. Because shear rates beyond that producing the maximum aggregation reduce the level of aggregation, it is expected that both the rate of increase of the backscattered power and the power level at the plateau may reach a maximum and then drop as the postreduction flow rate is further increased.

Kinetics of RBC aggregation for S_{10} = 32.2

As reported in Figs. 3 and 5, unexpected power variations were observed following flow reductions for S_{10} = 32.3. Additional results, not reported here because they were performed using a slightly different experimental protocol, provided similar patterns of variation for S_{10} = 35.1 and 36.9. With the exception of the postreduction flow rate of 40 mL min^{-1}, the results of Fig. 5 are characterized by a rapid increase of the backscattered power (Phase 1), a slight reduction followed by a plateau (Phase 2), another rapid increase (Phase 3) and another plateau (Phase 4). Curiously, the power increased only by approximately 11 dB within 2 min, which is smaller than the power variations observed in Fig. 3 for S_{10} = 18.9 and 25.6 (16 and 18 dB, respectively). This observation can be explained by the fact that the prereduction flow rate of 1250 mL min^{-1} was probably not sufficient to disrupt all RBC rouleaux for S_{10} = 32.3 (according to Qin et al. 1998, the mean shear rate across the tube at 1250 mL min^{-1} was around 56 s^{-1}), thus reducing the range of variations observed following flow reductions. This is highlighted by the power level at t = 0, which was around 10 dB for S_{10} = 25.6 (Fig. 4) and around 25 dB for S_{10} = 32.3 (Fig. 5). In Fig. 5, it is expected that four phases of power variation would have occurred at a postreduction flow rate of 40 mL min^{-1} if recording was made over a longer period of time.

The mechanism responsible for the phasic power increases of Fig. 5 is complex and may be associated to the combined effects of RBC aggregate formation and long rouleau disorientation. To better understand the contribution of particle orientation on the backscattered power, experiments by Allard et al. (1996) and results shown in Fig. 6 are summarized here. In the study by Allard et al. (1996), a strong anisotropy of the ultrasound backscattered power was observed at the center of the tube under steady flow using carbon fibers. Because the backscattered power increased by 8 dB for insonation angles varying from 40° to 80°, it was postulated that the anisotropy was due to the coherent orientation of fibers with the flow field. In the present study, such an orientation was probably present before flow reductions. The power drops observed in Fig. 6 can, thus, be explained by a random disorientation of carbon fibers with respect to the ultrasound beam following sudden flow reductions.

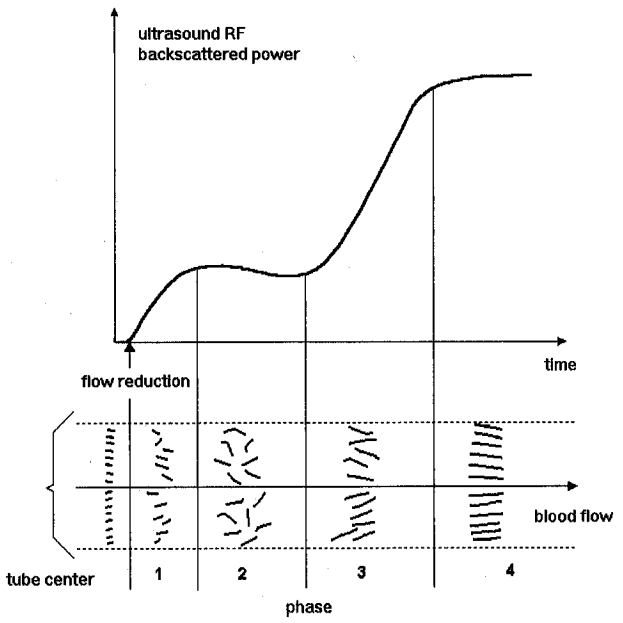

Fig. 7. Schematic representation of the relationship between the ultrasonic backscattered RF power and RBC rouleau formation, disorientation and reorientation for a horse blood model characterized by a high kinetics of rouleau formation.

When the flow was reduced, the fluid and suspended particles continued to move downstream because of the kinetic energy of the flow and sedimentation. It is postulated that flow disturbance and reverse flow may have contributed to the random disorientation of fibers all across the tube. As seen in Fig. 6, when the difference between the prereduction and postreduction flow rates was increased, the backscattered power reduction was more important, probably because of the presence of more significant disorientation and rotation of the fibers. The slight increases of the backscattered power following the first minimum are probably due to the reorientation of fibers under the new flow steady state or sedimentation effect.

According to this hypothesis, on the rheology of carbon fibers following flow reductions, it is plausible that RBC rouleau disorientation and reorientation with the flow contributed to the specific power variations observed in Fig. 5. It is clear from Fig. 6 that the disorientation of carbon particles reduces the backscattered power. The power increase to the first plateau followed by a slight reduction observed in Fig. 5 may, thus, be attributed to two opposing phenomena: increased RBC aggregation and rouleau disorientation. The schematic representation of the flow behavior of RBC rouleaux shown in Fig. 7 is used to support the following hypothesis. Before the sudden reduction of the flow, RBC rouleaux were relatively short and oriented with the

flow direction. When the flow rate was suddenly reduced, simultaneous RBC aggregation increase and rouleau disorientation occurred. Because rouleau formation had a dominant effect over rouleau disorientation in Phase 1, the backscattered power increased. An equilibrium between these two phenomena happened at the beginning of Phase 2. In the middle of Phase 2, the disorientation of rouleaux had a stronger effect and the power dropped slightly to reach a plateau. It is also possible that the rotation of rouleaux produced binding and breaking of large chains of RBCs. In Phase 3, rouleaux were reoriented with the flow field and continued to form, thus providing the second increase of the backscattered power until its final level (Phase 4). The time required for rouleau reorientation depended on the postreduction flow rate. As indicated by the duration of Phase 2, a higher postreduction flow rate reduced the time of rouleau reorientation because the step-down flow range was decreased, thus decreasing the flow field perturbation.

CONCLUSION

The variation within 2 min of the RF power backscattered by horse RBCs was investigated following a sudden flow stoppage or flow reductions from 1250 mL min^{-1} to 20–160 mL min^{-1}. It was shown that the backscattered power depended on the kinetics of rouleau formation and the postreduction flow rate. A specific pattern of variation of the backscattered power was found for hyperaggregating RBCs. The phasic increases of the backscattered power were attributed to the combined effect of RBC aggregate formation, random disorientation and reorientation with the flow.

The significance of this work in regard to human RBC aggregation kinetics is of several orders. First, this study increases the general understanding of the kinetics of RBC rouleau formation using a different species. Second, because horse RBCs can be used to simulate pathological levels of human RBC aggregation (Weng et al. 1996), the phasic power variations and explanation provided in Fig. 7 may exist in humans. Moreover, it is possible that a complete flow stoppage may not increase the backscattered power as a function of time under pathological human blood conditions. Thus, maintaining a postreduction flow rate instead of a complete flow stoppage may be more appropriate with human hyperaggregating RBCs. Further studies will have to be performed to confirm this hypothesis.

Acknowledgements—This work was supported by a research scholarship from the Fonds de la Recherche en Santé du Québec (G. C.), and by grants from the Medical Research Council of Canada (#MT-12491), the Whitaker Foundation, USA, and the Heart and Stroke Foundation of Quebec.

REFERENCES

Allard L, Cloutier G, Durand LG. Effect of the insonification angle on the Doppler backscattered power under red blood cell aggregation conditions. IEEE Trans Ultrason Ferroelec Freq Cont 1996;43:211–219.

Boynard M, Lelievre JC, Guillet R. Aggregation of red blood cells studied by ultrasound backscattering. Biorheology 1987;24:451–461.

Chen JF, Zagzebski JA. Frequency dependence of backscatter coefficient versus scatterer volume fraction. IEEE Trans Ultrason Ferroelec Freq Cont 1996;43:345–353.

Chien S. Electrochemical interactions between erythrocyte surfaces. Thrombosis Res 1976;8:189–202.

Cloutier G, Qin Z, Durand LG, Teh BG. Power Doppler ultrasound evaluation of the shear rate and shear stress dependences of red blood cell aggregation. IEEE Trans Biomed Eng 1996;43:441–450.

Copley AL, King RG, Huang CR. Erythrocyte sedimentation of human blood at varying shear rates. In: Grayson J, Zingg W, eds. Microcirculation. New York: Plenum Press, 1976:133–134.

Donner M, Siadat M, Stoltz JF. Erythrocyte aggregation: Approach by light scattering determination. Biorheology 1988;25:367–375.

Hoskins PR, Loupas T, McDicken WN. A comparison of the Doppler spectra from human blood and artificial blood used in a flow phantom. Ultrasound Med Biol 1990;16:141–147.

Kim SY, Miller IF, Sigel B, Consigny PM, Justin J. Ultrasonic evaluation of erythrocyte aggregation dynamics. Biorheology 1989;26:723–736.

Kitamura H, Sigel B, Machi J, Feleppa EJ, Sokil-Melgar J, Kalisz A, Justin J. Roles of hematocrit and fibrinogen in red cell aggregation determined by ultrasonic scattering properties. Ultrasound Med Biol 1995;21:827–832.

Mottley JG, Miller JG. Anisotropy of the ultrasonic backscatter of myocardial tissue: I. Theory and measurements in vitro. J Acoust Soc Am 1988;83:755–761.

Qin Z, Durand LG, Cloutier G. Kinetics of the "black hole" phenomenon in ultrasound backscattering measurements with red blood cell aggregation. Ultrasound Med Biol 1998;24:245–256.

Shung KK, Reid JM. Ultrasonic instrumentation for hematology. Ultrasonic Imaging 1979;1:280–294.

Weng X, Cloutier G, Pibarot P, Durand LG. Comparison and simulation of different levels of erythrocyte aggregation with pig, horse, sheep, calf, and normal human blood. Biorheology 1996;33:365–377.

Weng X, Cloutier G, Roederer GO, Beaulieu R. Contribution of acute-phase proteins and cardiovascular risk factors to erythrocyte aggregation in normal and hyperlipidemic individuals. (Abst.) Circulation 1997;96:I–251.

APPENDIX

As demonstrated in previous studies (Hoskins et al. 1990; Chen and Zagzebski 1996), the backscattered power from small particles is linear with the particle density at low volume fractions. This observation was used to calibrate the electronic circuits of the Doppler ultrasound system and compare the power measured using the quadrature Doppler signals and the RF signal. Polystyrene microspheres (Duke Scientific, Palo Alto, CA, 4–150 μm diameter) at concentrations varying between 0.05 and 2 g L^{-1} were suspended in a water-glycerol mixture (60% saline water, 40% glycerol) and circulated within a Kynar tube placed horizontally in a water bath. Ultrasound measurements were performed at the center of the tube at an angle of 45° and a mean flow rate of 400 mL min^{-1}. Doppler signals were digitized for 10 s using the method described in Qin et al. (1998), whereas RF data were collected over a period of 20 s using the approach described before. For both signals, the power (in relative units), was expressed as a function of the concentration of polystyrene microspheres in grams per liter of liquid. The range of variations of the power differed for both signals because of differences in the signal-processing methods used to compute the backscattered power. To facilitate the comparison of the results, the power of the RF signal was scaled to that of the Doppler

signal. The ratio of the power measured with the Doppler and RF methods, at a microsphere concentration of 1.1 g L^{-1}, was used as a scaling factor to obtain a similar range of variation of the power for concentrations varying between 0.05 and 2.2 g L^{-1}. Linear regression models were used to fit the data obtained from five series of measurements performed under the same experimental conditions. As shown in Fig. 8, the correlation coefficients (r^2) were similar, with values of 99.3% and 98.8% for the Doppler and RF signals, respectively. Both Doppler and RF electronic circuits had a satisfactorily linear response over the range of backscattered power measured in the current study.

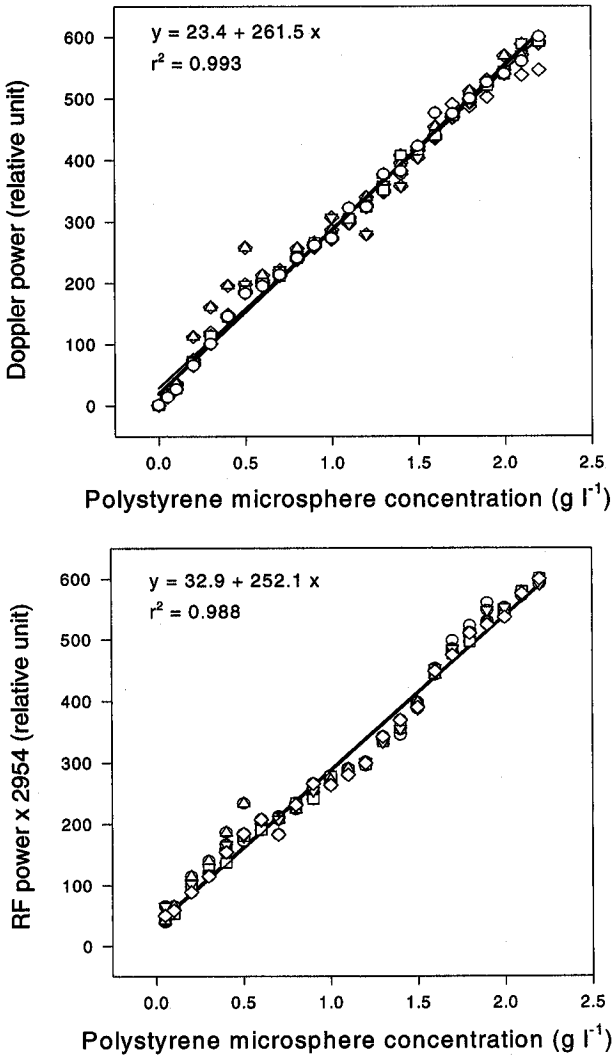

Fig. 8. Linear regressions used to assess the amplitude linearity of the Doppler (top) and RF (bottom) signals. Experiments were performed by circulating polystyrene microspheres at different concentrations in a steady flow model. The data were obtained from 5 series of measurements represented by □, ◇, △, ○, and ▽.